Physikalisch-Technische Bundesanstalt
Nationales Metrologieinstitut

On the techniques for primary calibration of electronic radon detectors

Mitev, K.[1]; Sabot, B.[2]; Todorov, V.[1]; Georgiev, S.[1]; Pierre, S.[2]; Röttger, S.[3]; Krastev, B.[1,4]; Dimitrova, I.[1]

[1] Sofia University "St. Kliment Ohridski", Faculty of Physics, 5 James Bourchier Blvd, 1164, Bulgaria
[2] Université Paris-Saclay, CEA, LIST, Laboratoire National Henri Becquerel (LNE-LNHB), F-91120, Palaiseau, France
[3] Physikalisch-Technische Bundesanstalt (PTB), Bundesallee 100, 38116, Braunschweig, Germany
[4] Department of Radiotherapy, University Oncology Hospital "Prof. Ivan Chernozemski", 1756, Sofia, Bulgaria

DOI: https://doi.org/10.1016/j.apradiso.2025.112209

Veröffentlichungsjahr: 2025

Acknowledgement: (z. B. der Förderung)

This work is supported by the project RadonNET (23IND07), which received funding by the European Partnership on Metrology (ID: 10.13039/100019599), co-financed from the European Union's Horizon Europe Research and Innovation Programme and by the Participating States. This work is supported by the European Union NextGenerationEU, through the National Recovery and Resilience Plan of the Republic of Bulgaria, project No BG-RRP-2.004-0008-C01. K.M.'s experimental work at PTB was made possible by a visit as a PTB visiting scientist, with financial support from PTB. This support is gratefully acknowledged.

Zitierform:

K. Mitev, B. Sabot, V. Todorov, S. Georgiev, S. Pierre, S. Röttger, B. Krastev, I. Dimitrova,

On the techniques for primary calibration of electronic radon detectors,

Applied Radiation and Isotopes,

Volume 226,

2025,

112209,

ISSN 0969-8043,

https://doi.org/10.1016/j.apradiso.2025.112209.

(https://www.sciencedirect.com/science/article/pii/S0969804325005548)

Applied Radiation and Isotopes 226 (2025) 112209

Contents lists available at ScienceDirect

Applied Radiation and Isotopes

journal homepage: www.elsevier.com/locate/apradiso

On the techniques for primary calibration of electronic radon detectors

K. Mitev [a], B. Sabot [b], V. Todorov [a], S. Georgiev [a], S. Pierre [b], S. Röttger [c], B. Krastev [a,d], I. Dimitrova [a,*]

[a] Sofia University "St. Kliment Ohridski", Faculty of Physics, 5 James Bourchier Blvd, 1164, Bulgaria
[b] Université Paris-Saclay, CEA, LIST, Laboratoire National Henri Becquerel (LNE-LNHB), F-91120, Palaiseau, France
[c] Physikalisch-Technische Bundesanstalt (PTB), Bundesallee 100, 38116, Braunschweig, Germany
[d] Department of Radiotherapy, University Oncology Hospital "Prof. Ivan Chernozemski", 1756, Sofia, Bulgaria

ARTICLE INFO

Keywords:
Radon
Low-activity calibration
Electronic monitors
Background build-up
RadonEye +2

ABSTRACT

Successful calibration of RadonEye +2 electronic radon detectors was performed at typical indoor activity concentrations using the facilities at LNHB and PTB. The calibration uncertainties using primary radon activity standards were: below 1.5 % at 300 Bq/m^3, below 1.7 % at 130 Bq/m^3 and below 2.5 % at 55 Bq/m^3 ($k = 1$). When using the secondary standard AlphaGUARD, the uncertainty at 55 Bq/m^3 was below 3.5 %. Maintaining stable activity concentrations proved crucial and appears to be the only feasible approach for calibrations below 100 Bq/m^3. While calibration under exponentially decaying radon activity concentration remains useful for evaluating the devices' linearity across a broad range, it proved unsuitable for calibration of user-grade monitors at low activities due to the high statistical variation in their signal.

The linearity of RadonEye +2 was demonstrated in the range 50 Bq/m^3 - 300 Bq/m^3 and they will be utilized for the sensor networks developed within the RadonNET project. Dynamic background correction, applicable to non-spectrometric detectors, was applied based on the monitor's exposure history. Furthermore, it was observed that the pulse-processing algorithm of RadonEyes +2 distorts the Poisson distribution of the signal, thereby increasing its variation. Potentially, lower measurement uncertainty could be achieved with electronic radon detectors that report the registered pulses and allow access to their processing algorithms.

1. Introduction

The need to reduce human exposure to radon (^{222}Rn), in order to lower the incidence of lung cancer, is recognized by authorities in many countries. Most have established reference levels for the annual average radon concentration, typically ranging from 100 Bq/m^3 to 400 Bq/m^3 in homes and from 100 Bq/m^3 to 1000 Bq/m^3 in workplaces, depending in some cases on the workplace occupancy (WHO). The WHO recommends that, where feasible, countries set the national reference level at 100 Bq/m^3 (World Health Organization, 2009). To identify buildings at risk or to confirm that mitigation efforts have successfully reduced radon levels, detectors must be capable of reliable measurements at these concentrations.

In the past decade electronic radon detectors (ERDs) targeted towards end-users, like homeowners and employers, have spread in the market and are quickly gaining popularity. Several laboratory studies on the metrological characteristics of different types of user-grade ERDs were published (Beck et al., 2024; Daraktchieva et al., 2024; Rey et al., 2024), showing that some commercial ERDs are suitable for measuring radon concentrations in dwellings and workplaces. Some of the devices have sufficiently fast response time of the order of a few hours (Dimitrova et al., 2023; Beck et al., 2024) to allow following radon dynamics. Such studies are valuable for improving exposure estimates (Turtiainen 2021; Venoso et al., 2021; Dimitrova et al., 2025b), for optimizing radon mitigation (Valcarce et al., 2022) and for understanding radon behavior indoors and outdoors. The outdoor radon monitoring is of interest not only for improving dose estimation (Petermann and Hofmann, 2025), but also because of the possibility to use radon as a tracer in atmospheric transport processes (see Curcoll et al., 2024 and the references therein) and ground-level emissions of greenhouse gases (Levin et al., 1999; Vogel et al., 2012; Wada et al., 2013).

This article is part of a special issue entitled: ICRM 2025 published in Applied Radiation and Isotopes.

* Corresponding author.
E-mail address: divelina@phys.uni-sofia.bg (I. Dimitrova).

https://doi.org/10.1016/j.apradiso.2025.112209
Received 28 June 2025; Accepted 24 September 2025
Available online 25 September 2025

For the abovementioned applications it is essential to develop and test comprehensive calibration procedures at activity concentrations below 100 Bq/m^3, allowing to calibrate ERDs, to test their range and linearity and to study the sources of uncertainty and potential bias of the measurements in this range. Currently, the lowest reported activity concentration at which performance tests of user-grade ERDs were made is 100 Bq/m^3 (Beck et al., 2024).

This work presents successful calibrations of RadonEye +2 ERDs at activity concentrations down to 50 Bq/m^3 with two different exposure systems, both of which use primary and secondary radon standards. The challenges of calibrating commercial ERDs at low radon concentrations are two types: those related to the creation and evaluation of the referent activity concentration (see Beck and Biel, 2024; Röttger et al., 2025) and those related to evaluation of the net signal of the monitors. Our work addresses both challenges, with more focus on the second group, which are further exacerbated by the black-box nature of the studied devices, for which the registered pulses and pulse-processing algorithms are unknown. Different exposure strategies were tested and evaluated. The results were further used to estimate the linearity of RadonEye +2 at low activity concentrations.

2. Materials and methods

2.1. Exposure modes

ERD calibrations were conducted in both dynamic and static modes. In dynamic mode the activity concentration should change very little within the response time of the ERD (Dimitrova et al., 2024). Such slow change can be realized by allowing radon to decay or build-up naturally in a hermetic vessel. In decay mode it is sufficient to introduce activity (traceable to a gas standard) in the exposure vessel with traceable volume and to verify the hermeticity. The build-up mode employs a radium (^{226}Ra) source with a traceable radon emanation rate connected to a traceable hermetic volume during the whole exposure. The source emanation rate should be stable for the given exposure conditions (e.g. temperature, humidity, flow rate) or should be measured during the exposure. Alternatively, a calibrated radon monitor can serve as a secondary standard and follow the activity change in dynamic mode even in systems with small non-hermeticity. Calibrations of ERDs at dynamic mode have been successfully carried out before (Dimitrova et al., 2024) in the range 280 Bq/m^3 – 2900 Bq/m^3, while simultaneously testing the linearity of the devices.

Exposures at static mode require maintaining constant activity concentration and a radium source. One option is to allow radon to build-up naturally in a closed volume until it reaches equilibrium with radium. The closed volume could be the exposure vessel or another volume which is later connected to the exposure vessel in a closed system. The activity concentration created in this mode is traceable through the source emanation rate and the volume of the system. It is also fixed by these two quantities (e.g. 100 Bq source is needed to create 100 Bq/m^3 in a 1 m^3 chamber). Another option is to continuously pass air with a constant flow rate through the radium source and the exposure vessel in an open system. By varying the flow rate, a wider range of concentrations can be achieved (the equations describing the evolution of radon can be found, for example, in Pressyanov et al., 2017). Traceability can be achieved by securing traceability of the source emanation rate, the flow rate and the calibration volume or by using a calibrated monitor as a secondary standard. An advantage of the static mode exposures is that they allow studying the statistical variations of the signal of ERDs, many of which do not report measurement uncertainty or counting rate.

All of the above modes were tested, namely: dynamic mode by decay and build-up and static mode in closed and open system. Their applicability to calibration of user-grade ERDs at activity concentrations below 100 Bq/m^3 was evaluated.

2.2. Exposure systems and conducted exposures

The first series of exposures involved 6 RadonEye +2 monitors (RE) and were conducted at LNHB (Laboratoire National Henry Becquerel), France at the facility for the production of reference atmosphere of radioactive gases (Sabot et al., 2020). Details about the reference activity concentrations, the exposure duration and conditions are given in Table 1. Two exposures (No 1 and 2 in Table 1) were conducted at decay mode in which radon activity of the order of several kBq/m^3 was introduced and closed in the exposure chamber until it decayed to background levels. The introduced activity was certified by the LNHB primary defined solid-angle ^{222}Rn standard (Sabot et al., 2016b). The volume of the exposure chamber is 0.1255 (5) m^3 and is traceable to volume standard calibrated by the French Metrology Institute. The free volume in the chamber was not measured for each exposure, but an absolute uncertainty of 0.1 L was introduced to the volume to account for the displaced volume of the REs.

Two other exposures (No 3 and 4) were conducted in an open system at constant radon activity concentration. The activity was introduced using a dry air flow regulated by a mass flow controller with a relative standard uncertainty of 0.1 %. The flow passes through a ^{226}Ra source with activity known with a relative standard uncertainty of 0.8 %. Its emanation was measured at 1.000 (1) with the primary thoron standard detector (Sabot et al., 2016a) developed at LNHB during the MetroRADON project (MetroRADON, 2023). The mass flowmeter has a response time of less than 100 ms ensuring a constant regulation of the flow rate with a stability below 0.1 % and a measurement uncertainty of 0.1 %, the standard deviation of the measured values over 3 days is typically 0.01 % ensuring a very stable flow rate over long periods.

Measurements of the RE background were conducted for 39 days immediately before the start of the first exposure in radon-free atmosphere produced by flushing the volume for 3 days with aged air at 20 L/min and then isolating the circuit. The background was checked again after the end of the first exposure.

The second exposure series were conducted at PTB (Physikalisch-Technische Bundesanstalt), Germany and the achieved activity concentrations are presented in Fig. 1. Three REs were exposed in a ~0.5 m^3 chamber along with an AlphaGUARD monitor. Some other large volume radon detectors were connected in a closed loop to the exposure chamber and the total volume of the system was 0.6744 (15) m^3. The displaced volume of the detectors inside the exposure system was estimated at less than 0.1 L and is negligible part of the total volume. The background of the devices was estimated before and after the first exposure in a radon-free atmosphere created by aged synthetic air. In the first exposure (No 5) constant radon activity was achieved by fast introduction of activity in the system from a different volume, in which radon and radium were already in equilibrium. After the source was connected to the exposure system, the air inside was homogenized by using a membrane pump with a flow rate of about 2 L/min through the source loop. The external detectors were operated with an additional membrane pump at a flow rate of about 1 L/min. The background and leakage of the whole system had been tested using synthetic, aged air from a 50 L, 200·10^3 hPa canister at a flow rate of 5 L/min controlled by a Bronkhorst mass flow controller, while observing the pressure. The other exposures (No 6 and 7) were in build-up mode in which radon activity coming from an open radon-emanating source is allowed to build-up in the closed volume until it reaches its plateau. The plateau region was selected to start 25 days after the exposure began, corresponding to 99 % of the maximum ^{222}Rn activity concentration. The exposure was then continued at constant activity concentration. In exposure No 7 an activity concentration of 55.56 (60) Bq was maintained for more than two months (Fig. 1).

The reference activity concentration in the first exposure at PTB was estimated based on the AlphaGUARD measurements. In the other exposures IRSDs (Integrated Radon Source Detectors) were used, which served as primary standards for absolute radon emanation (Mertes et al.,

Table 1
Description of the conducted calibration exposures of RadonEye +2 ERD.

No	Lab	Exp. Volume, m^3	Mode	Radon activity traceability	Referent Activity Conc., Bq/m^3	Duration, days	t, °C	RH, %	p, hPa
1	LNHB	0.125	dynamic, decay	primary, solid-angle meas.	4478 (30)	38	23.0 (15)	26.5 (9)	981 (5)
2	LNHB	0.125	dynamic, decay	primary, solid-angle meas.	6789 (42)	85	23.6 (10)	36.6 (9)	1067 (5)
3	LNHB	0.125	static, open	primary – source emanation rate	608.8 (49)	6	22.7 (9)	11.76 (38)	992 (5)
4	LNHB	0.125	static, open	primary – source emanation rate	304.4 (24)	6	22.8 (7)	11.441 (31)	991.2 (19)
5	PTB	0.674	static, closed	secondary, AlphaGUARD	239.6 (64)	4	24.41 (14)	24.01 (22)	1001.7 (39)
6	PTB	0.674	static, closed	primary, IRSD emanation rate	134.4 (15)	31	24.39 (13)	23.013 (41)	1022 (6)
7	PTB	0.674	static, closed	primary, IRSD emanation rate	55.56 (60)	>60	24.83 (6)	21.73 (28)	1006 (12)

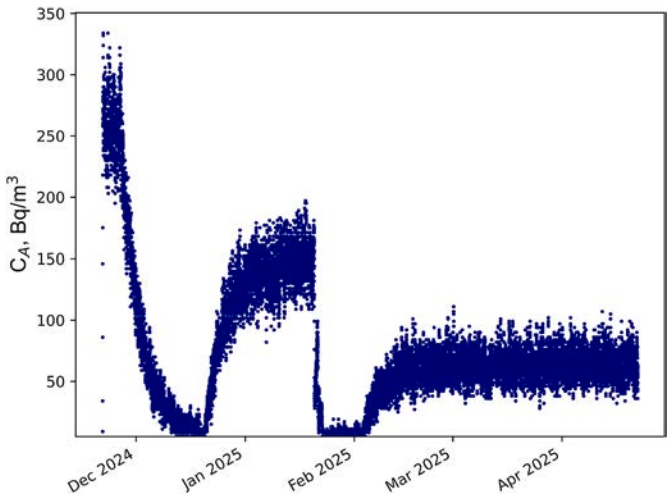

Fig. 1. RadonEye +2 ERD signal during three calibration sessions at PTB with regions of constant ^{222}Rn activity concentrations of 239.6 (64) Bq/m^3, 134.4 (15) Bq/m^3 and 55.56 (60) Bq/m^3. The lowest value is maintained constant for more than 2 months.

2023). The sources are produced in PTB by thermal physical vapor deposition of $^{226}RaCl_2$ onto ion-implanted silicon detector (Mertes et al., 2022). The spectrometric detector in the IRSD simultaneously determines the activity of ^{226}Ra and ^{222}Rn retained in the source and estimates the emanating radon activity as a function of time (see Fig. 2). The uncertainty of the emanating activity is also estimated dynamically. The counting efficiency of the source is close to 0.5 and is determined with an uncertainty of about 1 % (Mertes et al., 2022). The production method and the high efficiency of the IRSDs have allowed the characterization of low activity sources (Rottger et al., 2023). In the current work, sources with activity of 158.6 (1.7) Bq and 66.4 (5) Bq were used. Details about the reference activity concentration and the exposure conditions are given in Table 1.

The hermeticity of the exposure chambers was additionally tested during the exposures by fitting the signal of the RE monitors with the expected decay or growth curves of radon, respectively: $C_A = C_{A,0}\exp(-\lambda t)$ and $C_A = C_{A,max}(1-\exp(-\lambda t))$, where C_A is the activity concentration of radon, $C_{A,0}$ its initial value and $C_{A,max}$ its value at saturation. The fits were used to estimate the parameter λ and to compare it with the radon decay constant of 0.007554 (2) h^{-1} (Be et al., 2008). A good fit with a higher λ indicates constant-rate leakage from the exposure system. For the exposures at constant activity concentration the RE signal was fitted with a linear function and the slope was compared to 0. A negative slope could also indicate non-hermeticity of the system.

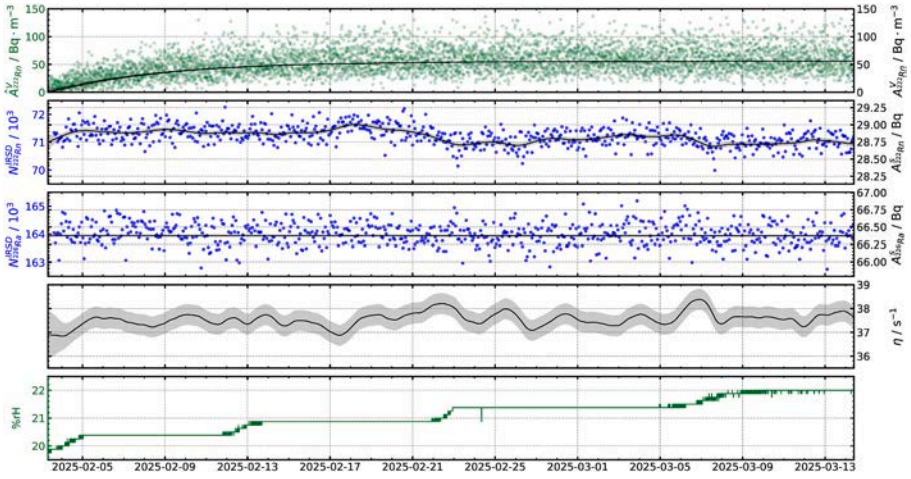

Fig. 2. Quasi online calculation of the IRSD emanation during exposure No 7 at PTB. The curves (top to bottom) show: the activity concentration by emanating radon (black curve) and the AlphaGUARD independent data (green dots); the radon activity retained in the source (black curve) and the corresponding number of nuclei (blue dots); the radium activity of the source (black curve) and the corresponding number of nuclei (blue dots); the calculated number of radon atoms η released per second with its uncertainty at 1σ (shaded interval) and the relative humidity as determined by the AlphaGUARD. (For interpretation of the references to colour in this figure legend, the reader is referred to the Web version of this article.)

2.3. RadonEye +2 monitors

The user-grade ERDs are compact devices with inner chambers of the order of a few hundred cm^3 in which radon enters by diffusion. Radon progeny in the air is stopped from entering by a passive filter. The alpha particles emitted in the chamber are registered by a semiconductor Si detector or pulsed ionization chamber. The sensitivity (k) of an ERD can be defined as the ratio of the net counting rate n_{net} and the true ^{222}Rn activity concentration in the air C_A:

$$k = \frac{n_{net}}{C_A}. \quad (1)$$

The sensitivity of the user-grade detectors is limited by their small volume. The REs used in the current work are produced by FTLab, South Korea and are based on a 200 cm^3 pulsed ionization chamber. They have one of the highest declared sensitivities among similar devices (Beck et al., 2024) – 1.35 counts per minute per 100 Bq/m^3, corresponding to combined counting efficiency of the alpha particles of ^{222}Rn, ^{218}Po and ^{214}Po of about 1.1. Most user-grade ERDs, including RE, cannot differentiate between alpha-particles with different energies and their background signal is increased by ^{210}Po decaying in the chamber.

The RadonEye +2 were chosen for this first test, because they have shown excellent performance in laboratory tests and field studies. The RE monitors were shown to be linear in the range 280 Bq/m^3 – 2900 Bq/m^3 (Dimitrova et al., 2024) and to have lower sensitivity at high radon activity concentrations (Turtiainen et al., 2021; Dimitrova et al., 2023). The linearity of REs at activity concentrations down to 100 Bq/m^3 was confirmed in another study (Beck et al., 2024). RadonEyes were successfully compared to passive track-etch radon detectors produced by the UK Health Security Agency (UKHSA) in a year-long study in occupied homes and workplaces in Bulgaria (Dimitrova et al., 2025a). The influence of environmental factors on the RE signal was studied in Beck et al. (2024a) for three devices. It was found that a temperature of 35 °C can lead to 30 % decrease in sensitivity compared to this at 20 °C. The sensitivity in dry air was found to be 6 %–7 % higher than that at 50 %–60 % relative humidity. An increase in sensitivity of 5 %–6 % per 100 hPa was also observed. In the current work, the values of the environmental parameters were controlled in all exposures and their dispersion was much smaller than the above differences (see Table 1).

In 2022 when the RE monitors used in the current study were new, their background was measured in nitrogen atmosphere. It was estimated to be 2.5 (5) Bq/m^3 for a batch of 20 devices. After that, all devices were used to monitor radon in dwellings or workplaces and in the process some of them were exposed to average activity concentrations reaching several kBq/m^3. In the brief periods when they were not used, REs were stored at low-radon atmosphere in a hermetic container. Thus, the predominant part of their radon exposure (from below 1 $MBq.h/m^3$ to over 30 $MBq.h/m^3$) was recorded and could be used for estimating their background.

The RadonEye +2 ERDs report the 60-min average of the radon activity concentration every 10 min over WiFi and record every sixth value in their memory. All reported values are rounded to an integer (in our settings in Bq/m^3). The monitors do not report the measurement uncertainty or the registered counts. The algorithms used to process the raw signal are also unavailable. In the conducted calibrations only independent measurements in consequent, non-overlapping 60-min intervals were used. We estimate a dimensionless correction factor as the ratio R of the reference activity concentration $C_{A,ref,net}$ and the RE-estimated activity concentrations $(C_{A,RE,net})$ corrected for background:

$$R = \frac{C_{A,ref,net}}{C_{A,RE,net}}, \quad (2)$$

The factor R serves as a multiplication correction. If $R < 1$, the sensitivity of the ERD k is higher than the one implemented in the algorithm of the device.

In our previous studies the statistical uncertainty of the single measurements of the REs was studied by analyzing data from long exposures (continuing for at least several days) at constant activity concentration. It was found that a semi-empirical formula could describe the standard deviation of the single measurement:

$$\sigma_{stat}(C_A) = \sqrt{\frac{C_{A,RE}}{k.\Delta t}}, \quad (3)$$

where $\Delta t = 60$ min is the single measurement interval and equivalent sensitivity of 0.69 (11) counts per minute per 100 Bq/m^3 was estimated for 9 monitors in the range 160 Bq/m^3 – 1800 Bq/m^3. In this work the variations of the signal were investigated down to 50 Bq/m^3.

2.4. Dynamic background correction

The build-up of ^{210}Pb in the non-spectrometric ERDs increases their background. Practically, all radon nuclei decaying in the chamber contribute to this build-up, since radon's short-lived progeny cannot leave the chamber. The product of ^{210}Pb (in the chain ^{210}Pb – ^{210}Bi - ^{210}Po), ^{210}Po, is an alpha-emitter and forms signal in the ionization chamber. Due to the long half-life of ^{210}Pb of 22.23 (12) years (Be et al., 2008), the background is in practice influenced by the whole exposure history of the detector. The use of a RE or another non-spectrometric ERD at low activity concentrations, whether in calibration or in field studies, requires dynamic estimate of the background. Using the exposure history, the background of each RE was estimated with 1 day resolution. The number of nuclei of ^{210}Pb generated per second was assumed equal to the radon activity inside the chamber. Then the activity of ^{210}Po inside the detector was expressed using the Bateman equations:

$$A_{Po-210} = \lambda_3 \sum_{t=1}^{t_{max}} R.\overline{C_{A,Rn}}(t).V.s\left(\prod_{i=1}^{2}\lambda_i\right)\sum_{j=1}^{3}\frac{\exp\left(-\lambda_j st\right)}{\prod_{k=1,k\neq j}^{3}\left(\lambda_k-\lambda_j\right)} \quad (4)$$

where the index t goes over each day of the detector history, R is the monitor correction factor given by Eq (2) and $\overline{C_{A,Rn}}$ is the daily average radon activity concentration reported by the monitor and recursively corrected for ^{210}Po contribution. The constant parameters used are the volume of the chamber $V = 2{\cdot}10^{-4}$ m^3, the seconds per day $s = 86\,400$ s and the decay constants in s^{-1} of ^{210}Pb, ^{210}Bi and ^{210}Po denoted by λ_1, λ_2 and λ_3, respectively. The contribution of the ^{210}Po activity to the background signal could be expressed as:

$$B_{Po-210} = \frac{\varepsilon_{Po-210}.A_{Po-210}}{k}, \quad (5)$$

where ε_{Po-210} is the unknown efficiency for registration of ^{210}Po in the chamber and k is the sensitivity in counts per second per Bq/m^3 used in the algorithm of the producer, which is also uncertain. These parameters could be estimated by measurements of the background, but several factors could lead to bias. These factors include: changes in the calibration factor of the monitor over time, missing records of exposure when the monitor is off, wrong zero records when the monitor is saturated and electronic noise contributing to the background. Therefore, we have used Eq (4) only to correct the measured values of the background to the time of the calibration exposure. In some cases, this correction was statistically significant, but did not exceed 20 %. The fact that the background could increase between different exposure sessions should be taken into account, especially in calibrations at low activity concentration.

3. Results

3.1. Hermeticity tests

Indication for non-hermeticity was found only in the first exposure in

decay mode (No 1). The rate of signal decrease λ of the 6 exposed REs was slightly, but systematically higher than the radon decay constant. Examples of fits are shown in Fig. 3. Different time intervals were tested (in the range of linearity of REs below 3000 Bq/m^3) and the value of λ = 0.00807 (12) h^{-1} was estimated. The referent activity concentration was then assumed to decrease with this rate and the uncertainty of the time correction was added to the uncertainty budget. The leakage was attributed to a defective valve of the system. In all other exposures, in which the activity changed with the decay rate of radon, this uncertainty component was neglected. An example of a linear fit during exposure at constant activity concentration is shown in Fig. 4. The results illustrate that despite the relatively high statistical uncertainty of the single RE measurements, they can be used for leakage tests.

3.2. RadonEye signal distribution

A new source of bias was identified by studying the distribution of the RE signal at background and constant-activity exposures – some integer values were never observed (visible as white horizontal lines in Fig. 4). The effect is clearly seen in histograms of the distribution in Fig. 5. It was noticed that the missing values were the same in the distributions for different session of the same detector. Some missing values were the same for different detectors and some were different. This discrete structure can be explained by looking at the distribution of pulses (N) registered for the duration of the ERD single measurement. The average number of pulses was deduced using Eq (1): $\overline{N} = n\Delta t = k.\overline{C_{A,RE}}\Delta t$. The sensitivity k in this case should be the one implemented in the algorithm of the device that is used to estimate the reported value of $C_{A,\,RE}$. It turned out that the value of k reported by the producer is too high to explain the gaps in the distribution. That is why, k was varied for each device. The average value $\overline{C_{A,RE}}$ was estimated both through the mean and the median of the $C_{A,\,RE}$ distributions. Then Poisson distributions of the pulses were obtained and converted back to histograms of the activity concentration $C_{A,\,RE}$. One of the distributions had the same average and the other had the same median as the experimental data. The modeled distributions were not rounded to integer $C_{A,\,RE}$ and are shown as dots in Fig. 5.

It can be seen that the rounding of the activity concentrations to the nearest integer can explain most of the missing points and the

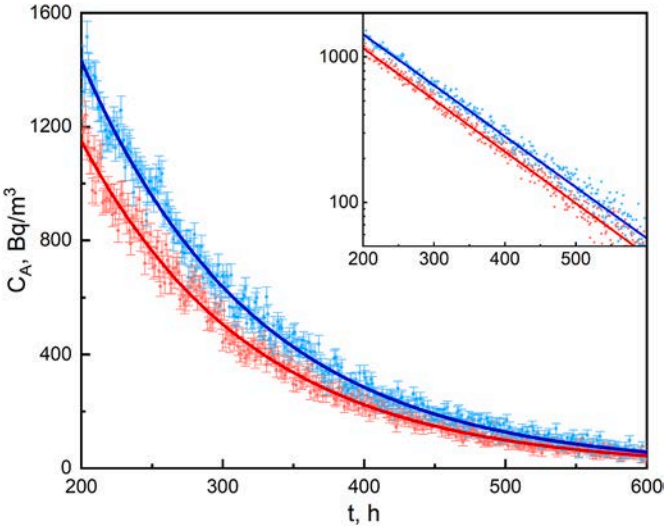

Fig. 3. Exponential fit with $C_A = C_{A0}$*exp(-λ *t) of the net signal of 2 RadonEye +2 during exposure No 1. They have different sensitivity, but close decrease rates (see the inset in log-scale). The parameter λ is 0.00818 (4) h^{-1} for the red curve and 0.00807 (4) h^{-1} for the blue curve. (For interpretation of the references to colour in this figure legend, the reader is referred to the Web version of this article.)

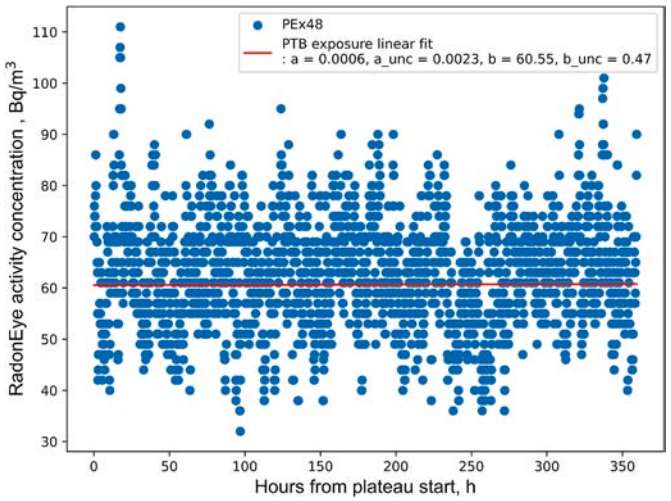

Fig. 4. Linear fit of the raw signal of a RadonEye during exposure No 7. The slope is zero within the estimated uncertainties.

distribution shape. However, in some cases (see Fig. 5b), additional spills of pulses in neighboring channels are observed leading to high peaks. This might be due to rounding from pCi/L to Bq/m^3 or to other filtering. It is not definite whether the distribution with the same mean or the same median describes the results better. In some cases, there is small difference between the means of the two distributions (within 2 Bq/m^3). In all cases, the experimental distributions had much bigger variation than what could be deduced from the Poisson distributions. This indicates that the pulse processing algorithm introduces variation in addition to the Poisson statistics. It also explains our previous results in which the standard deviation of the single measurement, estimated by Eq (3), corresponded to 2 times lower sensitivity than the declared value.

Similar distortion of the distribution can occur in all ERDs that round the activity concentration to integer. When the registered counting rates and the processing algorithm are unknown, the true distribution cannot be reconstructed. The possibility of a shift in the average value and the additional variation should be considered in low activity measurements and calibrations.

Further studies are planned for REs, but in the current calibrations an absolute uncertainty of ±1 Bq/m^3 was added to the signal to account for possible shifts in the average. The exposures at constant activity concentrations were used to estimate the single measurement standard deviations and to compare them with these given by Eq (3). The results in Table 2 show that Eq (3) gives adequate estimates down to 55 Bq/m^3 and that the REs signal variation has not changed significantly.

3.3. RadonEye +2 background

The background signal of the 9 studied REs ranged from 4.7 Bq/m^3 to 44 Bq/m^3. The background of the monitors studied at LNHB was statistically higher in the second blank session than in the first, which was 90 days earlier. This could be justified by the past exposure of the monitors as illustrated in Fig. 6. In the shown example, the integrated radon exposure accumulates until about a month before the calibration and the background signal continues to build during it. In Fig. 6 this signal is normalized to agree with the background measurement in January–February 2024. The signal in the initial background measurements (in 2021) could be due to some other source of background (e.g. electronic noise) or to unrecorded exposure during the storage of the new detector. The background measurements made in 2024 were corrected to account for the growth of background after this, using the estimated increase in the background (blue curve in Fig. 6). Similar estimates lead to corrections of up to 20 % in the background of the

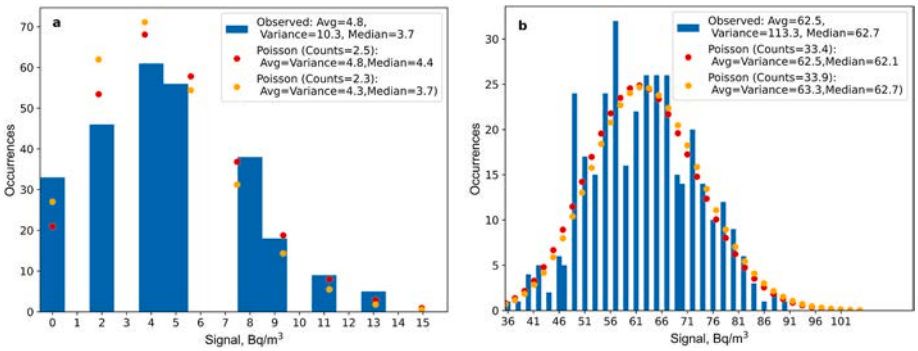

Fig. 5. Distribution of the reported values of a RadonEye +2 (only integers) in exposures to radon-free atmosphere (a) and to constant activity concentration (b). The dots are obtained from Poisson distribution of the pulses obtained by varying the sensitivity, so that the mean (red) or the median (yellow) are conserved. The dots correspond to integer number of pulses not rounded to integer activity concentration. (For interpretation of the references to colour in this figure legend, the reader is referred to the Web version of this article.)

Table 2
Relative standard deviation of the single measurements of REs exposed at different constant activity concentrations. The measured values of the relative standard deviation are compared with an empirical estimate by Eq (3).

	avg.CA, Bq/m^3		rel. St.dev C_A, %	
Detectror	referent	measured	measured	given Eq (3)
PEx25	608.8	941	6.5	5.1
PEx25	304.4	472	7.6	7.2
PEx41	239.6	274	14.5	9.4
PEx41	134.4	162	10.2	12.2
PEx41	55.56	69	18.4	18.7
PEx45	239.6	273	9.2	9.4
PEx45	134.4	156	11.0	12.5
PEx45	55.56	65	17.6	19.3
PEx48	239.6	251	15.1	9.8
PEx48	134.4	148	11.4	12.8
PEx48	55.56	62	17.1	19.7
PEx49	608.8	956	6.4	5.0
PEx49	304.4	496	8.4	7.0

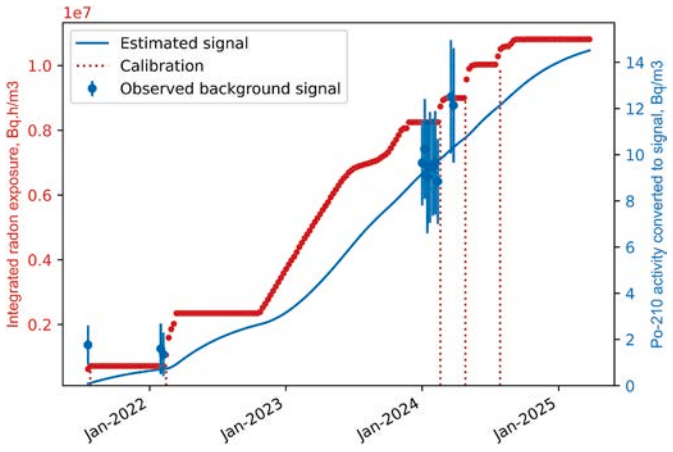

Fig. 6. Build-up of the total exposure of RE detector with time (red scale). The ^{210}Po activity is estimated by Eq (4) and converted to RE signal (blue scale), so that it agrees with the observed signal (dots) in Feb 2024. The starts of calibration exposures are marked (vertical dotted lines). The exposure in 2022–2023 is in a dwelling. (For interpretation of the references to colour in this figure legend, the reader is referred to the Web version of this article.)

detectors exposed in the subsequent sessions at LNHB (in July and August 2024). The relative uncertainty of the correction was assumed equal to the uncertainty of the correction factor R of 3.5 % (since the uncertainties of the other values in Eq. (4), like the times and the decay constants are much smaller) and had negligible contribution to the background uncertainty. The background corrections for the detectors exposed at PTB were smaller due to the shorter period between the background measurement and the exposures and the lower past exposures of the detectors.

3.4. Calibrations in dynamic mode

Calibrations at slowly changing activity concentrations have been successfully carried out previously in the range 280 Bq/m^3 – 2000 Bq/m^3 (Dimitrova et al., 2024). In the current study, RE time-stamped results were first synchronized in time with the referent activity concentration. When the referent value was provided by a detector (the IRSD or the AlphaGUARD), all referent values falling in the 60-min measurement interval of the RE were averaged. The referent activity range was split into smaller intervals. In the case of the two exposures in decay mode (No 1 and 2), the intervals were 20 Bq/m^3 wide above 300 Bq/m^3 and 5 Bq/m^3 wide below this value, to account for the slower absolute change in activity and higher standard deviations in the low range. For the two exposures in build-up mode (No 6 and 7) the intervals were 5 Bq/m^3 wide, but the interval corresponding to the plateau was dropped, so that it does not weight unproportionally. For each RE the measurements corresponding in time to the referent values falling in each interval were aggregated.

Fig. 7 shows an example of the box plot of the distributions of the RE signal at different intervals of referent values for exposure No 7 (e.g. the distribution of all RE values corresponding in time to referent values from 72.5 Bq/m^3 to 77.5 Bq/m^3 is represented by box, whiskers and outliers above the referent value 75 Bq/m^3). A linear fit of the data with the standard deviation of each distribution as weight is made. It is compared to the line obtained from the calibration of the same detector at the constant activity in the plateau (at 134.4 Bq/m^3) giving the slope a and the estimated background giving the free parameter b. Both lines visibly describe the data well and this is confirmed by the χ^2 test (the probabilities p not to reject the fit are close to 1). On the other hand, the slopes of the two fits differ significantly and lead to different calibration results. It follows that using dynamic calibration in the low activity range is not the best strategy and could lead to arbitrary results due to the high statistical fluctuations of the single measurements of the ERD.

In Fig. 8 the signal of a RE during the calibration at decay mode at LNHB is shown demonstrating the statistical variation in different activity regions. Similar statistical fluctuations can be expected from the other user-grade ERDs, because they have similar or lower sensitivity. Despite that dynamic mode calibrations are not suitable in the range below 100 Bq/m^3, they can be used to test the linearity of ERDs in a wide region. In Fig. 9 this is illustrated by plotting the correction factor R of a RE at different radon activity concentrations. As observed before, R

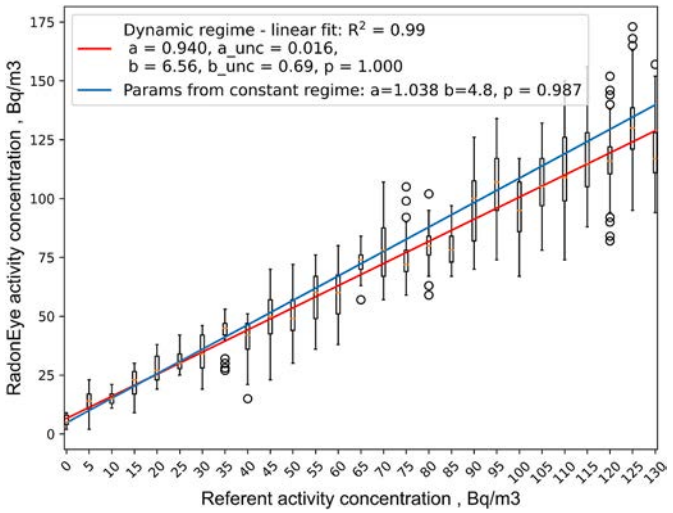

Fig. 7. Box plot of the distributions of the RE signal (no background correction) inside the corresponding referent activity concentration interval. The boxes represent the interquartile range and the circles the outliers that fall beyond 1.5 the interquartile range. The red line represents a linear fit of the data. The blue line is derived from the same RE calibration at 55 Bq/m3 (parameter a) and background measurement (parameter b). For the two lines a chi-square test gives the probability not to reject the fit p. (For interpretation of the references to colour in this figure legend, the reader is referred to the Web version of this article.)

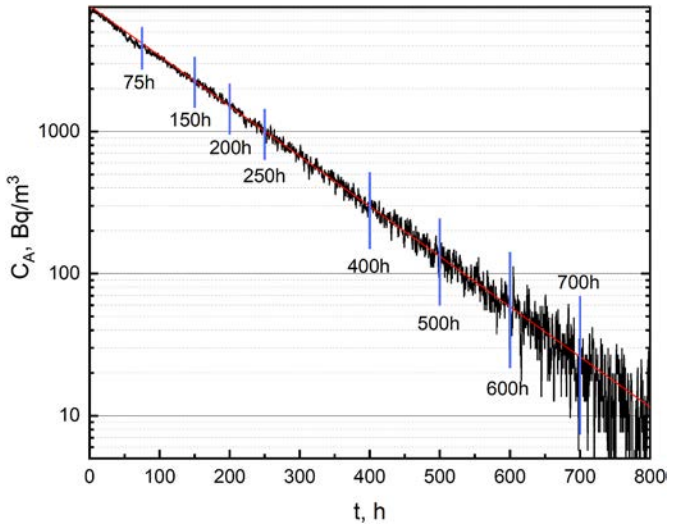

Fig. 8. Single 60-min RE measurements at decaying activity concentration (exposure No 1).

increases (i.e. sensitivity decreases) in the high activity region, which is probably due to the device dead time.

3.5. Calibrations at constant activity

The exposures at constant activity concentration (No 3–7) were used to estimate the correction factor *R* using the reference values provided by the primary and the secondary standards. The averages of the measured activity concentration were corrected for background as well as the reference values by the secondary standard (AlphaGUARD). Examples of the *R* values estimated in different exposure sessions are given in Fig. 10. It can be seen that the values at constant activity exposures carried out at PTB agree very well with each other (Fig. 10a). They demonstrate the linearity of the REs at activity concentrations down to

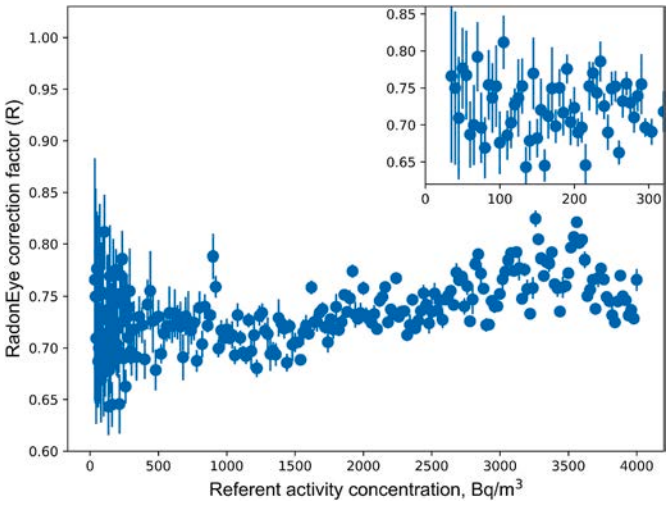

Fig. 9. Values of a RE correction factor in the range 30 Bq/m^3 - 4000 Bq/m^3 obtained in a calibration at decaying activity concentrations (exposure No 1).

50 Bq/m^3. The values at constant exposures at LNHB also agree within the declared uncertainties (Fig. 10b). It should be noted that the correction factors *R* of different RadonEye +2 devices can differ significantly (like the two shown in Fig. 10a and b) and that individual calibration of these devices is recommended, as shown in Dimitrova et al. (2024).

The uncertainty budget for all conducted exposures is presented in Table 3. Notably, calibration at 55 Bq/m^3 with overall uncertainty below 2.5 % (at 1 σ) was achieved with the IRSD standard at PTB. Using the AlphaGUARD monitor also lead to relatively low uncertainty of 3.4 % at 55 Bq/m^3. The uncertainty of the RE signal had the highest weight in the total uncertainty.

4. Conclusions

Successful calibration of RadonEye +2 electronic radon detectors was carried out at typical indoor radon concentrations using the facilities at LNHB and PTB to create constant activity concentrations. The achieved calibration uncertainties with primary radon activity standards were below 1.5 % at 300 Bq/m^3, below 1.7 % at 130 Bq/m^3 and below 2.5 % at 55 Bq/m^3 (1σ confidence interval). When using the AlphaGUARD as a reference monitor, the uncertainty at 55 Bq/m^3 was below 3.5 %. The dynamic mode (activity decay or build-up) proved unsuitable for calibration of user-grade ERDs in this activity range, because the high statistical variation of the ERD signal can justify different calibration factors. For RadonEye +2, which is among the most sensitive user-grade monitors on the market, the relative standard deviation was above 10 % below 100 Bq/m^3 and about 20 % at 55 Bq/m^3. While dynamic mode calibration remains useful for accessing ERD linearity in a broad range, exposure at stable constant activity seems to be the only viable option for studies below 100 Bq/m^3.

The linearity of RadonEye +2 in the range 50 Bq/m^3 - 300 Bq/m^3 was demonstrated. Dynamic background correction, universal for non-spectrometric detectors, was successfully applied to account for changes in the RE background between the calibration sessions. The correction relies on knowing the detector's exposure history, necessitating their storage in a low-radon atmosphere when switched off. Furthermore, it was found that the pulse-processing algorithm of RadonEyes +2 distorts the Poisson distribution of the signal and leads to additional variation. This implies that lower measurement uncertainty could be achieved with ERDs that report the registered pulses and allow access to their processing algorithms.

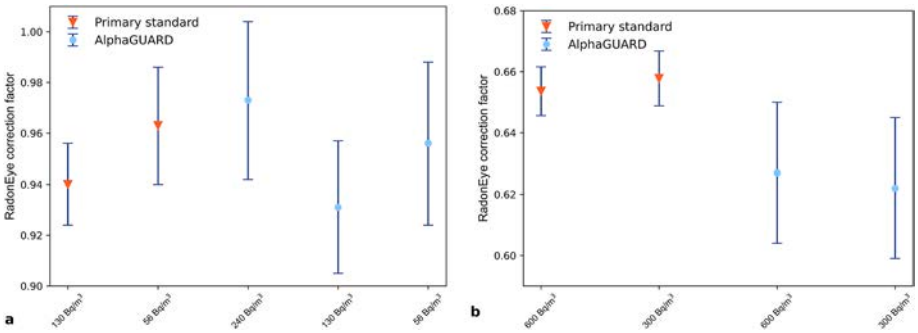

Fig. 10. The corrections factors *R* of ERDs obtained in different exposures: (a) RadonEye exposed in PTB and (b) RadonEye exposed in LNHB.

Table 3
Uncertainty budget of the conducted calibrations of RadonEye +2 ERDs.

Source	Uncertainty (k = 1)
Referent activity	
Rn standard rel. unc, %	Primary: LNHB: 0.8 %–1 %; PTB - IRSD: 1 %–1.2 %; Secondary: AlphaGUARD - 2.5 %
Volume rel. unc. , %	Primary: due to inactive volume of detectors: LNHB: 0.8 %; PTB:negligible Secondary: N/A
Decay correction	Hermetic volume: negligible; Non-hermetic: 1.5 %–7 % depending on time and decay rate unc. 1.5 %
Stat. unc	Primary: N/A; Secondary: AlphaGUARD - 1 % av. st. dev. At 55 Bq/m^3
RadonEye	
Stat. unc	Dynamic mode: fit slope unc.: 0.5 %–1 %; Static mode: av. st. dev.: <1 % at 300 Bq/m^3 for 6 days, <2 % at 55 Bq/m^3 for 15 days
Channel cross-talk abs. unc, Bq/m^3	1 Bq/m^3 (to be refined)
RadonEye background abs. unc., Bq/m^3	Due to stat. unc. and build-up correction: 0.1 Bq/m^3 - 0.6 Bq/m^3; Due to channel cross-talk: 1 Bq/m^3
Total	At 50 Bq/m^3 - 2000 Bq/m^3: 1 %–2 % (LNHB, primary, hermetic); At 300 Bq/m^3: 1.3 %–1.4 % (LNHB, primary); 3.7 % (LNHB, secondary); At 130 Bq/m^3: 1.6 %–1.7 % (PTB, primary); 2.8 % (PTB, secondary); At 55 Bq/m^3: 2.3 %–2.4 % (PTB, primary); 3.4 % (PTB, secondary)

CRediT authorship contribution statement

K. Mitev: Conceptualization, Methodology, Project administration, Writing – review & editing, Formal analysis, Investigation. **B. Sabot:** Investigation, Methodology, Resources, Writing – review & editing. **V. Todorov:** Data curation, Investigation, Validation. **S. Georgiev:** Formal analysis, Investigation, Visualization, Writing – review & editing. **S. Pierre:** Investigation, Writing – review & editing, Validation. **S. Röttger:** Formal analysis, Investigation, Methodology, Writing – review & editing, Resources. **B. Krastev:** Investigation, Validation. **I. Dimitrova:** Data curation, Methodology, Visualization, Writing – original draft, Writing – review & editing.

Declaration of competing interest

The authors declare that they have no known competing financial interests or personal relationships that could have appeared to influence the work reported in this paper.

Acknowledgements

This work is supported by the project RadonNET (23IND07), which received funding by the European Partnership on Metrology (ID: 10.13039/100019599), co-financed from the European Union's Horizon Europe Research and Innovation Programme and by the Participating States. This work is supported by the European Union NextGenerationEU, through the National Recovery and Resilience Plan of the Republic of Bulgaria, project No BG-RRP-2.004-0008-C01. K.M.'s experimental work at PTB was made possible by a visit as a PTB visiting scientist, with financial support from PTB. This support is gratefully acknowledged.

Data availability

Data will be made available on request.

References

Be, M.M., Chiste, V., Dulieu, C., Browne, E., Chechev, V., Kuzmenko, N., Kondev, F., Luca, A., Galan, M., Pearce, A., Huang, X., 2008. Monographie BIPM-5: Table of Radionucleides, vol. 4. Bureau International des Poids et Mesures, France. https://www.bipm.org/en/publications/monographies. ISBN: 92-822-2230-6.

Beck, T.R., Foerster, E., Biel, M., Feige, S., 2024. Measurement performance of electronic radon monitors. Atmosph 15 (10), 1180. https://doi.org/10.3390/atmos15101180.

Beck, T.R., Biel, M., 2024. Metrological realization of the radon activity concentration in air. Apl. Radiat. Isot. 212, 111448. https://doi.org/10.1016/j.apradiso.2024.111448.

Curcoll, R., Grossi, C., Röttger, S., Vargas, A., 2024. Full characterization and calibration of a transfer standard monitor for atmospheric radon measurements. Atmos. Meas. Tech. 17, 3047–3065. https://doi.org/10.5194/amt-17-3047-2024.

Daraktchieva, Z., Howarth, C.B., Wasikiewicz, J.M., Miller, C.A., Wright, D.A., 2024. Long-term comparison and performance study of consumer grade electronic radon integrating monitors. J. Radiol. Prot. 44, 031508. https://doi.org/10.1088/1361-6498/ad66db.

Dimitrova, I., Georgiev, S., Mitev, K., Todorov, V., Dutsov, C., Sabot, B., 2023. Study of the performance and time response of the RadonEye Plus2 continuous radon monitor. Measure 207, 112409. https://doi.org/10.1016/j.measurement.2022.112409.

Dimitrova, I., Georgiev, S., Todorov, V., Daraktchieva, Z., Howarth, C.B., Wasikiewicz, J. M., Sabot, B., Mitev, K., 2024. Calibration and metrological test of the RadonEye Plus2 electronic monitor. Radiat. Meas. 175, 107169. https://doi.org/10.1016/j.radmeas.2024.107169.

Dimitrova, I., Wasikiewicz, J.M., Todorov, V., Georgiev, S., Daraktchieva, Z., Howarth, C. B., Wright, D.A., Sabot, B., Mitev, K., 2025a. Coherent long-term average indoor radon concentration estimates obtained by electronic and solid state nuclear track detectors. Radiat. Phys. Chem. 226, 112212. https://doi.org/10.1016/j.radphyschem.2024.112212.

Dimitrova, I., Todorov, V., Georgiev, S., Mitev, K., 2025b. Real time monitoring of Rn-222 in workplaces and estimation of working time correction factor. Radiat. Meas. 181, 107359. https://doi.org/10.1016/j.radmeas.2024.107359.

Levin, I., Glatzel-Mattheier, H., Marik, T., Cuntz, M., Schmidt, M., Worthy, D.E., 1999. Verification of German methane emission inventories and their recent changes based on atmospheric observations. J. Geophys. Res. Atmos. 4, 3447–3456. https://doi.org/10.1029/1998JD100064.

Mertes, F., Röttger, S., Röttger, A., 2022. Development of ^{222}Rn emanation sources with integrated quasi 2π active monitoring. Int. J. Environ. Res. Publ. Health 19, 840. https://doi.org/10.3390/ijerph19020840.

Mertes, F., Röttger, S., Röttger, A., 2023. Approximate sequential Bayesian filtering to estimate ^{222}Rn emanation from ^{226}Ra sources usinR spectral time series. Journal of Sensors and Sensor Systems 12 (1), 147–161. https://doi.org/10.5194/jsss-12-147-2023.

MetroRADON, 2023. Research summary of the EMPIR MetroRADON project. Appl. Radiat. Isot. 193, 110672. https://www.sciencedirect.com/science/article/pii/S0969804323000258.

Petermann, E., Hoffmann, B., 2025. Mapping the exposure to outdoor radon in the German population. J. Environ. Radioact. 281, 107583. https://doi.org/10.1016/j.jenvrad.2024.107583.

Pressyanov, D., Mitev, K., Georgiev, S., Dimitrova, I., Kolev, J., 2017. Laboratory facility to create reference radon + thoron atmosphere under dynamic exposure conditions. J. Environ. Radioact. 166 (1), 181–187. https://doi.org/10.1016/j.jenvrad.2016.03.018.

Rey, J.F., Meisser, N., Licina, D., Goyette Pernot, J., 2024. Performance evaluation of radon active sensors and passive dosimeters at low and high radon concentrations. Build. Environ. 250, 111154. https://doi.org/10.1016/j.buildenv.2023.111154.

Röttger, S., Röttger, A., Mertes, F., Morosch, V., Balle, T., Chambers, S., 2023. Evolution of traceable radon emanation sources from MBq to few Bq. Appl. Radiat. Isot. 196, 110726. https://doi.org/10.1016/japradiso.2023.110726.

Röttger, S., Röttger, A., Mertes, F., Chambers, S., Griffiths, A., Curcoll, R., Grossi, C., 2025. Traceable low activity concentration calibration of radon detectors for climate change observation networks. Measure: Sensors (Peterb., NH), 101708. https://doi.org/10.1016/j.measen.2024.101708.

Sabot, B., Pierre, S., Michielsen, N., Bondiguel, S., Cassette, P., 2016a. A new thoron atmosphere reference measurement system. Appl. Radiat. Isot. 109, 205–209. https://doi.org/10.1016/j.apradiso.2015.11.055.

Sabot, B., Pierre, S., Cassette, P., 2016b. An absolute radon 222 activity measurement system at LNE-LNHB. Appl. Radiat. Isot. 118, 167–174. https://doi.org/10.1016/j.apradiso.2016.09.009.

Sabot, B., Rodrigues, M., Pierre, S., 2020. Experimental facility for the production of reference atmosphere of radioactive gases (rn, Xe, Kr, and H isotopes). Appl. Radiat. Isot. 155, 108934. https://doi.org/10.1016/j.apradiso.2019.108934.

Turtiainen, T., Kojo, K., Laine, J.-P., Holmgren, O., Kurttio, P., 2021. Improving the assessment of occupational exposure to radon in above-ground workplaces. Radiat. Protect. Dosim. 196 (1–2), 44–52. https://doi.org/10.1093/rpd/ncab127.

Valcarce, D., Alvarellos, A., Rabuñal, J.R., Dorado, J., Gestal, M., 2022. Machine learning-based radon monitoring system. Chemosensors 10, 239. https://doi.org/10.3390/chemosensors10070239.

Venoso, G., et al., 2021. Impact of temporal variability of radon concentration in workplaces on the actual radon exposure during working hours. Sci. Rep. 11, 16984. https://doi.org/10.1038/s41598-021-96207-9.

Vogel, F.R., Ishizawa, M., Chan, E., Chan, D., Hammer, S., Levin, I., Worthy, D.E.J., 2012. Regional non-CO2 greenhouse gas fluxes inferred from atmospheric measurements in Ontario, Canada, J. Integr. Environ. Sci. 9, 41–55. https://doi.org/10.1080/1943815X.2012.691884.

Wada, A., Matsueda, H., Murayama, S., Taguchi, S., Hirao, S., Yamazawa, H., Moriizumi, J., Tsuboi, K., Niwa, Y., Sawa, Y., 2013. Quantification of emission estimates of CO2, CH4 and CO for east Asia derived from atmospheric radon-222 measurements over the Western north Pacific. Tellus B 65, 1–16. https://doi.org/10.3402/tellusb.v65i0.18037.

WHO. National reference levels, data by country. Available online. https://apps.who.int/gho/data/view.main.RADON03v (Accessed April 2025).

World Health Organization, 2009. WHO handbook on indoor radon - a public health perspective. https://www.who.int/publications/i/item/9789241547673.